

# Hygroscopic growth and water uptake kinetics of two-phase aerosol particles consisting of ammonium sulfate, adipic and humic acid mixtures

S. Sjogren<sup>a</sup>, M. Gysel<sup>a</sup>, E. Weingartner<sup>a,\*</sup>, U. Baltensperger<sup>a</sup>, M.J. Cubison<sup>b,1</sup>, H. Coe<sup>b</sup>, A.A. Zardini<sup>c</sup>, C. Marcolli<sup>c</sup>, U.K. Krieger<sup>c</sup>, T. Peter<sup>c</sup>

<sup>a</sup>Laboratory of Atmospheric Chemistry, Paul Scherrer Institut, CH-5232 Villigen, Switzerland

<sup>b</sup>School of Earth, Atmospheric and Environmental Science, University of Manchester, Manchester, UK

<sup>c</sup>Institute for Atmospheric and Climate Science, ETH, Zurich, Switzerland

Received 7 July 2006; received in revised form 14 November 2006; accepted 15 November 2006

---

## Abstract

The hygroscopic growth of solid aerosol particles consisting of mixtures of ammonium sulfate and either adipic acid or Aldrich humic acid sodium salt was characterized with a hygroscopicity tandem differential mobility analyzer and an electrodynamic balance. In particular, the time required for the aerosol particle phase and the surrounding water vapor to reach equilibrium at high relative humidity (RH) was investigated. Depending on the chemical composition of the particles, residence times of > 40 s were required to reach equilibrium at 85% RH, yielding up to a 7% reduction in the measured hygroscopic growth factors from measurements at 4 s residence time compared to measurements at equilibrium. We suggest that the solid organic compound, when present as the dominant component, encloses the water-soluble inorganic salt in veins and cavities, resulting in the observed slow water uptake. Comparison with predictions from the Zdanovskii–Stokes–Robinson relation shows enhanced water uptake of the mixed particles. This is explained with the presence of the salt solution in veins resulting in a negative curvature of the solution meniscus at the opening of the vein. In conclusion, it is important for studies of mixtures of water soluble compounds with insoluble material to allow for sufficient residence time at the specified humidity to reach equilibrium before the hygroscopicity measurements.

© 2006 Elsevier Ltd. All rights reserved.

**Keywords:** HTDMA; EDB; ZSR; Hygroscopicity; Mass transfer limitation; Kelvin effect

---

## 1. Introduction

Aerosol particles in the atmosphere affect the earth's radiation balance in various ways (IPCC, 2001). Firstly, aerosol particles absorb and scatter radiation. This *direct aerosol effect* is influenced by the hygroscopicity of the aerosol

---

\* Corresponding author.

E-mail address: [ernest.weingartner@psi.ch](mailto:ernest.weingartner@psi.ch) (E. Weingartner).

<sup>1</sup> Now at: Cooperative Institute for Research in Environmental Science, University of Colorado, Boulder, USA.

particles, which is determined mainly by their chemical composition. Secondly, the tendency for cloud formation and resulting cloud properties similarly depends on the chemical composition as well as on the size distribution of the aerosol particles (e.g. McFiggans et al., 2006). Thus, the cloud albedo and the radiative properties of cloud droplets are influenced, coined the *indirect aerosol effect*.

Atmospheric aerosol components can be classified into inorganic and organic components (e.g. Kanakidou et al., 2005). The hygroscopic properties of most inorganic salts present in the atmosphere are well known (e.g. Ansari & Pandis, 1999; Colberg, Luo, Wernli, Koop, & Peter, 2003). Of the many organic species identified in the aerosol (e.g. Putaud et al., 2004), the hygroscopic properties of quite a few pure substances have been characterized. However, to date the hygroscopic properties of only a few mixtures have been investigated. Inorganic salts (for instance ammonium sulfate (AS) and sodium chloride) can show a hysteresis behavior during uptake and loss of water, i.e. by exhibiting a difference between the deliquescence and efflorescence relative humidities (DRH/ERH), and with a higher water content of the deliquesced than the effloresced particles in this relative humidity (RH) range. Conversely, organic constituents of the aerosol without hysteresis behavior can contribute to an uptake of water at lower RH than the DRH of inorganic salts. This has been reported by Dick, Saxena, and McMurry (2000) and is also theoretically expected, as such complex mixtures can remain in the liquid state and exchange water with the gas phase at lower RHs (Marcolli, Luo, & Peter, 2004).

The response of aerosol particles to changes in RH can be measured by a variety of instruments. The particle levitation technique using an electrodynamic balance (EDB) has been demonstrated to be a valuable method for studying the hygroscopic properties of single aerosol particles (Davis, Buehler, & Ward, 1990). This technique has the advantage that the particle mass can be monitored continuously as a function of RH, thus providing unambiguous in situ characterization of the particle mass growth due to water uptake. It can be used for particles with diameters larger than a few micrometers. A different method for characterizing water uptake is the hygroscopicity tandem differential mobility analyzer (HTDMA, Rader & McMurry, 1986).

In this paper, measurements performed by two HTDMAs are compared with each other and with results obtained with an EDB. One of the HTDMAs is from the University of Manchester (UMan), UK (Cubison, Coe, & Gysel, 2005), the other one from the Paul Scherrer Institute (PSI), Switzerland (Weingartner, Gysel, & Baltensperger, 2002), while the EDB is from ETH Zurich (Colberg, Krieger, & Peter, 2004). Hygroscopicity measurements for a variety of mixtures are presented. The growth of AS is compared with the theoretical prediction using the aerosol diameter-dependent equilibrium model (ADDEM) (Topping, McFiggans, & Coe, 2005a, 2005b) developed at the UMan. In the case of mixtures of different components (AS with organics), the hygroscopic growth was predicted using the Zdanovskii–Stokes–Robinson (ZSR) relation for water activities of mixed particles (Stokes & Robinson, 1966).

Mass transfer effects in hygroscopic measurements of aerosol particles have recently obtained more attention. It has been discussed whether organic/inorganic aerosol mixtures show mass transfer limitations of water (contrary to pure inorganic salts which equilibrate very fast, within timescales of  $< 1$  s). Kerminen (1997) considered the gas-phase transfer to particles before cloud activation, and reported calculated equilibration times  $< 1$  s. However, a field study by Chuang (2003) found that a fraction of the particles exhibited a slower water uptake than the majority of particles sampled, which was explained by a low mass accommodation coefficient in that study. Chan and Chan (2005) did a review of the different hygroscopicity studies with possible mass transfer effects for water uptake of aerosol particles, concluding the need for further investigation. Cubison (2005) described an experimental set-up and results for several systems. Our study further investigates and analyzes the results from measurements with varying residence times at elevated RH. In order to evaluate the water vapor equilibration time, the residence time of the particles at high RH was varied from seconds to minutes.

AS was chosen as the inorganic salt in this study, as its hygroscopicity is well known and it is a common constituent in the atmosphere. Adipic acid (AA) was chosen as an organic constituent. AA has a low vapor pressure and is only moderately soluble in water (high DRH). At the RHs studied here it is present in its crystalline form, which is assumed to contribute to a prolonged water uptake equilibration time. AA has also been identified in atmospheric samples (Ray & McDow, 2005). Furthermore tests were carried out with the commercially available Aldrich humic acid sodium salt (NaHA). This compound serves as a proxy for humic-like substances that were identified as a major component of the isolated organic matter in the atmospheric aerosol (Graber & Rudich, 2006; Kiss, Tombacz, Varga, Alsberg, & Persson, 2003).

## 2. Experimental methods

### 2.1. Hygroscopic growth and the ZSR relation

The hygroscopic growth (GF) indicates the relative increase in mobility diameter of particles due to water absorption at a certain RH, and is defined as

$$\text{GF}(\text{RH}) = \frac{D(\text{RH})}{D_0}, \quad (1)$$

where  $D(\text{RH})$  is the mobility diameter at a specific RH and  $D_0$  is the dry particle mobility diameter measured for spherical particles (dynamic shape correction factor,  $\chi$ , is 1). Near-sphericity ( $\chi < 1.01$ ) was ensured by choosing  $D_0$  either as the smallest diameter measured during hydration mode (see Section 2.2), or, if the aerosol showed water uptake at low RH, by choosing the diameter extrapolated to 0% RH for the dehydration mode (droplets). Mobility GFs obtained with an HTDMA are only equal to volume equivalent GFs if the particles do not change the shape during water uptake. The GF is presented in humidograms (i.e. showing the response in hygroscopic growth versus RH).

The hygroscopic GF of a mixture ( $\text{GF}_{\text{mixed}}$ ) can be estimated from the GFs of the pure components and their respective volume fractions,  $\varepsilon$ , with the ZSR relation (Gysel et al., 2004; Stokes & Robinson, 1966)

$$\text{GF}_{\text{mixed}} = \left( \sum_k \varepsilon_k \text{GF}_k^3 \right)^{1/3}, \quad (2)$$

where the summation goes over all compounds present in the particles. The model assumes spherical particles, ideal mixing behavior (i.e. no volume change upon mixing) and independent water uptake of the organic and inorganic components. The volume fractions for the two components in the dry particles were calculated as

$$\varepsilon_i = \frac{(w_i/\rho_i)}{\sum_k (w_k/\rho_k)}, \quad (3)$$

where  $w_i$  is the mass fraction and  $\rho_i$  the density of the pure substance  $i$ . Values of  $\rho$  used in the model were 1.77, 1.36 and 1.1 g/cm<sup>3</sup> for AS, AA and NaHA, respectively, obtained from the product suppliers. The hygroscopic growth of AS was parameterized for the deliquesced state from our measurements, between 35% and 93% RH, with

$$\text{GF} = (1 - \%RH/100)^\gamma + c, \quad (4)$$

where RH is given in percent, and the coefficients  $\gamma$  and  $c$  were fitted as  $-0.21821$  and  $0.070$ , respectively. The standard deviation of the residuals between this parameterization and the ADDEM model was 0.012 in GF (Topping et al., 2005a).

### 2.2. HTDMA

The two HTDMAs employed (from UMan and PSI) are operated in a similar manner. A differential mobility analyzer (DMA1) selects a monodisperse aerosol size,  $D_0$ , under dry conditions (RH < 10%). The aerosol then passes through a humidifier with a controlled higher RH, and the diameter  $D$  is measured with a second DMA (DMA2). A scheme can be seen in Fig. 1. The two DMAs are similar to the TSI 3071 type. The instrument from PSI with a closed-loop sheath air uses only the aerosol flow entering the DMA2 to regulate the RH in the DMA2. The RH of the sheath air thus follows the RH of the aerosol flow. RH setpoint changes were kept small, in order to maintain similar RH in the aerosol flow as in the sheath air. In this study data were used only if the variation in the sheath air was < 1% RH during each scan.

The UMan instrument humidifies the aerosol flow and the sheath air flow with two independent humidifiers and controllers. The RH of the aerosol and the sheath air was kept identical. The two DMAs used were constructed in house and are of the Vienna design (Winklmayr, Reischl, Lindner, & Berner, 1991).

Both HTDMAs were kept at a constant temperature set in the range 18–23 °C (controlled by a water bath). A few degrees cooling of DMA2 with respect to the aerosol and sheath air conditioners (at constant laboratory temperature)

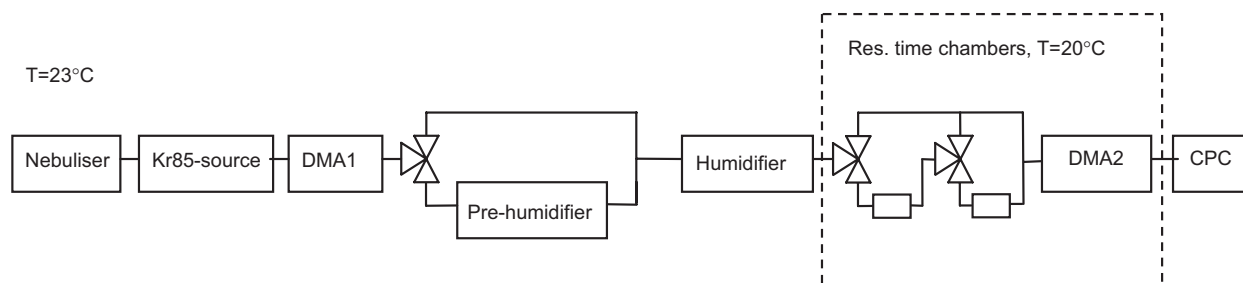


Fig. 1. Experimental set-up of the HTDMA.

was necessary to reach high RHs ( $> 90\%$  RH). The relevant RH in DMA2 was determined by measurement of the system temperature and the DMA2 excess sheath air dew point using a dew point mirror. The accuracy of the RH measurement at higher RH is for example  $90 \pm 1.2\%$ , assuming no temperature gradients in the DMA2. The hygroscopic GF can be determined with a precision ( $2 \times$  standard deviation) of  $\Delta\text{GF} \approx \pm 0.01$  (at  $D_0$ ) and  $\Delta\text{GF} \approx \pm 0.03$  (at DRH). Measurements of solid inert material, such as mineral dust, performed with the same HTDMA set-up show a precision of  $\Delta\text{GF} \approx \pm 0.005$  (see Vlasenko et al., 2006).

Two different ways to operate the HTDMA were used; these are denoted hydration and dehydration mode. For the hydration mode, the mono-modal dry particles were exposed to a monotonically increasing RH until the size measurement in DMA2. For the dehydration mode the particles were first deliquesced at  $\text{RH} > 80\%$  in a pre-humidifier, and then the RH was monotonically lowered to the RH in DMA2, thus allowing the ERH to be measured. For the ERH measurements the DMA2 was kept at a temperature similar to the laboratory temperature in order to guarantee that the lowest RH behind the pre-humidifier occurs in DMA2, to avoid efflorescence before DMA2. The pre-humidifier switched on/off automatically. This setup allows a completely automated operation of the HTDMA.

### 2.3. Residence time chambers

In order to study the effect of residence time of the aerosol in the HTDMAs, chambers of different volumes were installed after the humidifier (before entry to DMA2), allowing the aerosol to equilibrate at the specified RH for a range of residence times. The chambers were kept at the same temperature as the DMA2 in order to ensure constant RH from the chambers to DMA2. The chambers were of different sizes yielding measured residence times ( $\tau_{\text{res}}$ ) ranging from 3 s to 2 min in total. The errors in  $\tau_{\text{res}}$  were on the order of  $\pm 4$  s for  $\tau_{\text{res}} < 30$  s and  $\pm 11$  s for  $\tau_{\text{res}} \geq 30$  s. The geometries of the chambers were chosen as cylinders with a ratio of length to diameter of about 3–10, because of space availability and construction reasons. Several measurement scans, each with a duration varying between 1 and 3 min, were done after switching to the chamber with the longest  $\tau_{\text{res}}$  to allow for a steady state to build up. Then, monotonically shorter  $\tau_{\text{res}}$  were measured (by turning three-way valves), until only connecting tubing was used for the shortest  $\tau_{\text{res}}$ . If the pre-humidifier was used, the  $\tau_{\text{res}}$  was increased by 10 s (time from the middle of the pre-humidifier to the main humidifier). The residence times stated below are thus from the middle of the first humidifier (pre-humidifier or main humidifier) through the tubing and residence chambers up to the entry point of the sheath air inside the DMA2. The time from the entry point of DMA2 to where the aerosol flow mixes with the sheath air is 3.5 s for the PSI HTDMA and 2 s for the UMan HTDMA.

### 2.4. Electrodynamic balance

An electrically charged particle (typically 2–10  $\mu\text{m}$  in radius) is levitated in an EDB (Davis et al., 1990). The RH is set by adjusting the  $\text{N}_2/\text{H}_2\text{O}$  ratio of constant gas flow, using automatic mass flow controllers. During an experiment, the temperature is kept constant while the RH is changed with a constant rate. The sensor was calibrated directly in the trap using the DRH of different salts. Its accuracy is  $\pm 1.5\%$  RH between 10% RH and 80% RH and  $\pm 3\%$  RH above 80% RH.

To characterize the particle a HeNe laser (633 nm) illuminates the particle from below. The video image of the particle on a CCD detector and an automatic feedback loop are used to adjust the DC-voltage for compensating the

Table 1  
Substances used during the experiments

Substance	Purity	Producer	Product no.
Ammonium sulfate, MicroSelect	99.5	Fluka	09978
Adipic acid, Puriss	99.6	Riedel-deHaen	27635
Humic acid, sodium salt, tech. isolated from crude lignite	N.a.	Aldrich (purchased 2003)	H16752

gravitational force. A change in DC voltage is therefore a direct measure of the mass change. If the voltage at dry conditions ( $RH < 10\%$ ) corresponds to the dry mass of the particle ( $M_{dry}$ ) we can deduce the mass GF. In addition, we use a photomultiplier with a conical detection angle (approximately  $0.2^\circ$  half-angle) to measure the scattering intensity at  $90^\circ$  to the incident beam and feed this signal to an analog lock-in amplifier to measure the intensity fluctuations, that is, the root mean square deviation from the intensity mean (RMSD intensity). Because of its symmetry, a homogeneous spherical particle will show a constant scattering intensity and hence a very small fluctuation amplitude (corresponding to a value of 0.04, for our noise level). A non-spherical particle will scatter light with different intensity in the detection angle depending on its orientation relative to the incoming laser beam. All particles perform Brownian rotational motion in an EDB, which leads to an RMSD intensity between 0.5 and 5 depending on the deviation from spherical symmetry of the particle in its dry, solid state. We have used these intensity fluctuation amplitudes previously to characterize liquid microdroplets with a single solid inclusion (Krieger & Braun, 2001). In the following we will use this to identify the occurrence of phase transitions and to characterize the morphology of complex aerosol particles.

### 2.5. Aerosol generation/substances tested

Aerosol mixtures were generated using an atomizer (Type TSI 3076) operated with purified compressed air. Details on the substances investigated are found in Table 1. The substances were dissolved in MilliQ-water ( $18\text{ M}\Omega\text{ cm}$ ). All solutions appeared completely dissolved at visual inspection. It is assumed that the resulting aerosol was an internal mixture with the same mass ratio as in the solution, (cf. Gysel et al., 2004). This seems plausible, as no broadening of the GF distributions from the HTDMA could be detected while switching from the pure AS to the mixtures. The solutions were diluted further with MilliQ-water in the case the original solution yielded too high particle concentrations for the HTDMA at the size studied. The nebulized aerosol produced was subsequently dried in a silica gel diffusion dryer (residence time 30 s). It was found that the mixed aerosol was irregular in shape and restructured up to 5% in mobility diameter after deliquescence. These shape effects have been minimized by introducing a subsequent hydration/dehydration cycle ( $RH > 82\%$ ) to allow for deliquescence followed by efflorescence before the HTDMA. With this setup it was found that the particles did not restructure further in the HTDMA (within the instrument's precision), which indicates a more compact, spherical, shape. The dried particles were neutralized by means of a Kr-85 source and then fed into the HTDMA for the hygroscopicity measurement.

## 3. Results

### 3.1. Comparison of the two HTDMAs with pure AS

The sizing of the DMAs in both instruments was verified with polystyrene latex spheres in the size range from 90 to 400 nm. Thereafter instrument performance was verified by measurements of hygroscopicity of the ammonium sulfate (Fig. 2). AS is a well investigated substance and the two HTDMA instruments measured reproducible results ( $GF_{PSI} = 1.48$  and  $GF_{UMan} = 1.46$  at 80% RH and for  $D_0 = 100$  nm) which correspond well with literature (Gysel, Weingartner, & Baltensperger, 2002; Hennig, Massling, Brechtel, & Wiedensohler, 2005). The modeled curve is calculated as in Topping et al. (2005a). The calculated DRH of AS is 79.9% RH for large particles (Tang & Munkelwitz, 1993). As the particle diameter decreases, the DRH is theoretically predicted to increase. Deliquescence occurs when the free energy of the effloresced particle surface equals the free energy of the deliquesced particle. The surface energy increases with decreasing particle diameter, due to the Kelvin effect (Russell & Ming, 2002). A negligible increase is predicted for  $D_0 = 100$  nm particles. Moreover, a recent experimental study showed no significant increase of DRH

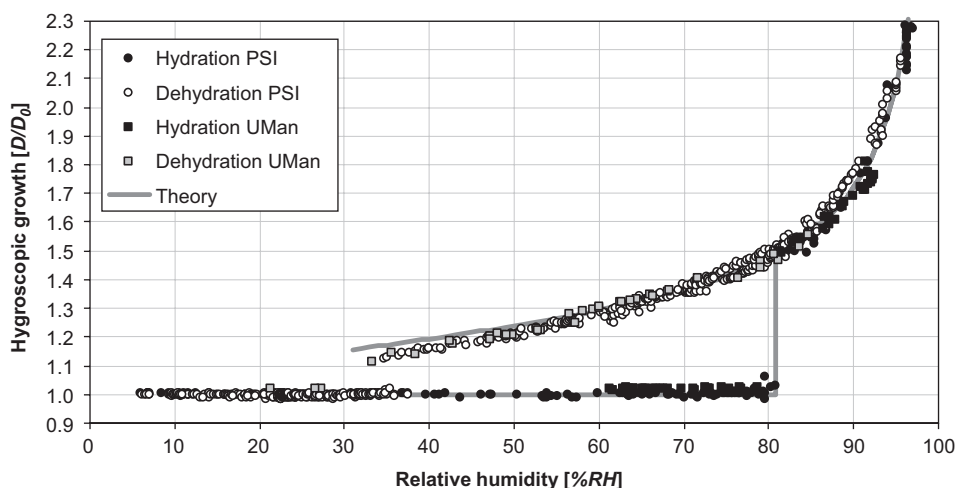


Fig. 2. Humidogram of laboratory-generated  $D_0 = 100$  nm ammonium sulfate aerosol from the two HTDMAs ( $T \sim 20^\circ\text{C}$ ). The two instruments show a good agreement.

for AS nanoparticles down to 6 nm (contrary to NaCl), within the range of RH uncertainty ( $\pm 2.5\%$  RH in that study) (Biskos, Paulsen, Russell, Buseck, & Martin, 2006). The PSI HTDMA measured a DRH of 80.5% RH (average of six measurements, standard deviation 0.75%,  $D_0 = 100$  nm), which is in the range of literature values reported. The  $\tau_{\text{res}}$  at the conditioned RH for different runs was varied between 4 and 40 s, and no influence of varying the  $\tau_{\text{res}}$  was detected. This confirms that equilibration of inorganic salts is fast,  $< 1$  s. Measurements of AS were done at the beginning of the intercomparison period and after regular intervals (about every 2 weeks) thereafter.

### 3.2. Hygroscopicity of pure adipic acid and pure humic acid

Pure adipic acid (AA) does not show any uptake of water (e.g.  $\text{GF} = 1.00 \pm 0.02$  up to 96% RH) (Joutsensaari, Vaattovaara, Vesterinen, Hämeri, & Laaksonen, 2001), which was confirmed up to RH 92% with both HTDMAs and the EDB in this study. AA is considered to be present as a crystalline solid in this study. This was confirmed with the two-dimensional angular scattering pattern from the EDB.

The hygroscopicity of pure NaHA has also been measured in two former studies (Badger et al., 2006; Gysel et al., 2004). Within experimental error, our results on the growth measured with the dehydration mode are comparable with these studies. However, measurements with the hydration mode differ at lower RH just outside the experimental error. This could be due to different morphology of the particles caused by differences in nebulizer conditions and/or drying conditions after the nebulizer. Particles composed of only NaHA showed no difference in GF as the residence time was varied at high RH. However, as the hygroscopicity of the NaHA is relatively low, the resolution of the HTDMA might not be sufficient to discern an effect for pure NaHA.

### 3.3. Hygroscopicity of AS/AA mixtures

The hygroscopic growth of four mixtures, with mass ratios of 1:1, 1:2, 1:3 and 1:4 AS/AA, were measured. In order to evaluate the equilibration time of the water uptake, the hygroscopic GF was measured with the HTDMAs at various residence times. The hygroscopic GFs of deliquesced particles measured in the RH range 70–95% (for the hydration mode data only above DRH was used) were interpolated with an empirical fit to 85% RH for each mixture and residence time. Most points were measured in the vicinity of 85% RH. Fig. 3 shows box plots of the determined GFs at 85% RH as a function of residence time for the 1:1, 1:2, 1:3 and 1:4 mixtures. The box plots consist of the mean GF (star), as well as 75/25 percentile (box) and 95/5 percentile (whiskers) of the residuals between the measurements and the fit line. Experimental uncertainties for the GF precision and  $\tau_{\text{res}}$  accuracy are as stated in Sections 2.2 and 2.3.

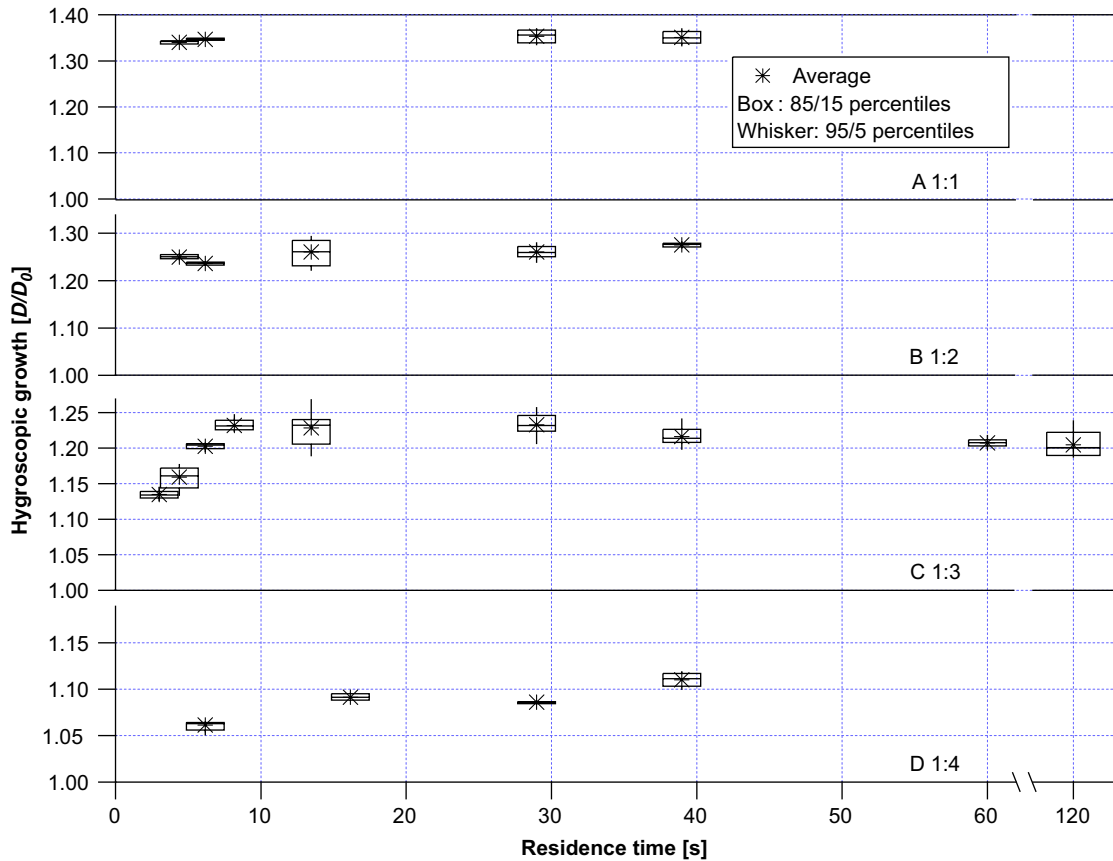


Fig. 3. Hygroscopic growth for AS/AA mass ratios 1:1, 1:2, 1:3 and 1:4 (top to bottom panel), measured with different residence times.  $D_0 = 100$  nm and GF relates to 85% RH. The 3 and 60 s residence time data for the AS/AA 1:3 mixture was measured with the UMan HTDMA, rest of data was measured with the PSI HTDMA. Each box represents on average 44 data points.

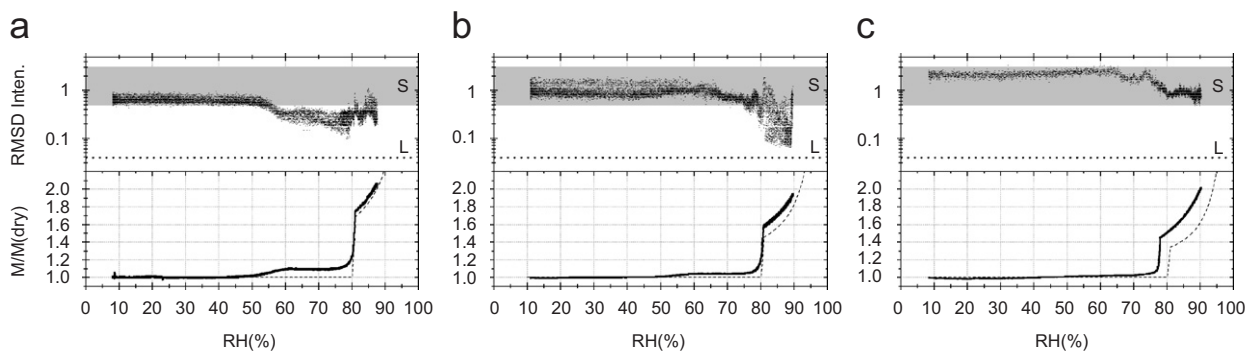


Fig. 4. Experimental hygroscopic mass growth ( $M/M_0$ , solid lines in lower panels) and ZSR model (dashed lines in lower panels) and intensity fluctuation data (RMSD intensity, upper panels) from EDB measurements for three mixtures of AS/AA: (a) 1:1 in mass ratio, (b) 1:2, (c) 1:3. The shaded area labeled (S) marks the RMSD intensities typical for a solid non-spherical particle, the line labeled (L) marks the RMSD intensity for a completely liquid and hence spherical particle. See text for details.

Figs. 4 (EDB) and 5 (HTDMA) show the humidograms of the AS/AA mixtures for residence times sufficiently long such that the equilibrium size is reached. In the ZSR relation AA was assumed solid, thus not contributing to the growth at all ( $GF = 1.0$  at any RH). The presence of AA as a solid was confirmed by intensity fluctuation data from

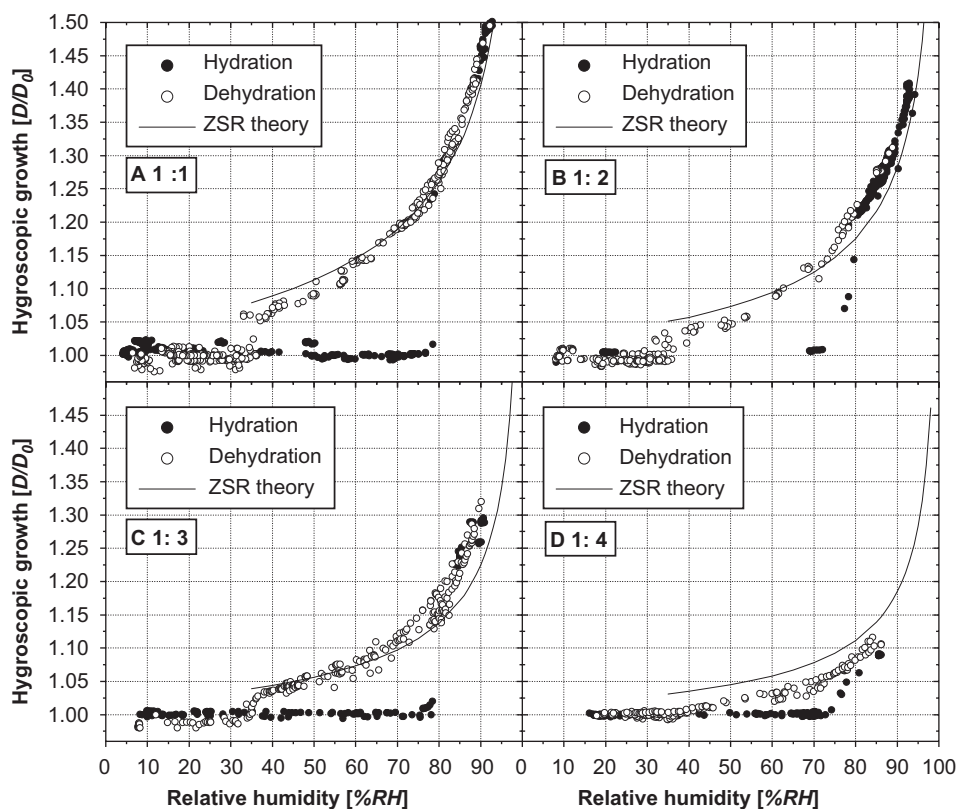


Fig. 5. Humidograms of ammonium sulfate-adipic acid mixtures AS/AA. Mass ratios are indicated by the labels A–D,  $D_0 = 100$  nm and data points were measured at equilibrium with both HTDMAs (data for AS/AA 1:4 at residence time > 30 s, see text).

EDB measurements shown in Fig. 4: all mixtures over the whole RH range show RMSD of scattered light intensity significantly above what is observed for completely liquid particles. Hence there was always a solid phase present in the particle. Note, however, that at RH substantially lower than the DRH of ammonium sulfate the intensity fluctuations decrease as a consequence of water uptake, leading to an optically more homogeneous spherical particle. The water uptake below ammonium sulfate DRH is clearly detected by the hygroscopic mass growth. At DRH of AS the intensity fluctuations stay constant or increase again (1:1 and 1:2 mixtures) because the water content is now large enough for Brownian motion of the solid adipic acid inclusion in the aqueous solution particle to occur.

There is a substantial deviation of hygroscopic GFs from ZSR prediction at RH above the DRH of ammonium sulfate for 1:2 and 1:3 mixtures, and a shift in DRH to lower RH. In 25 experiments with different particles of the 1:3 composition in the EDB we observed a scatter of values ranging from 1.16 to 1.45 in GF at DRH and a scatter ranging from 78% to 83% RH in DRH, which is significantly more scatter than instrument precision. This complex behavior of water uptake is most likely due to the morphology of the solid adipic acid (water uptake in confined spaces, e.g. grain boundaries), and it will be discussed to some extent in Section 4.2 and in more detail in a separate paper.

For the 1:1 and 1:2 AS/AA mixture, no increase in growth with longer residence time at high RH was noted for the interval studied here (4.4–40 s), as can be seen from the top two panels of Fig. 3. The hygroscopic growth of the 1:1 mixture is in good agreement with the ZSR approach (Figs. 4a and 5a) and with previous measurements (Hämeri, Charlson, & Hansson, 2002; Prenni, De Mott, & Kreidenweis, 2003).

In the HTDMA measurements of the 1:3 mixture, a dependence on residence time of the measured GF was observed, which was larger than the experimental precision (estimated as  $2 \times$  standard deviation), irrespective of the HTDMA instrument used (UMan or PSI). During the observable residence times (3–120 s) the GF increased from 1.15 to 1.24, reaching its equilibrium value after about 10 s (panel C in Fig. 3). For this mixture, the equilibrium hygroscopic growth exceeds the one predicted by the ZSR model by 0.08. This deviation is larger than the precision of the measurements,

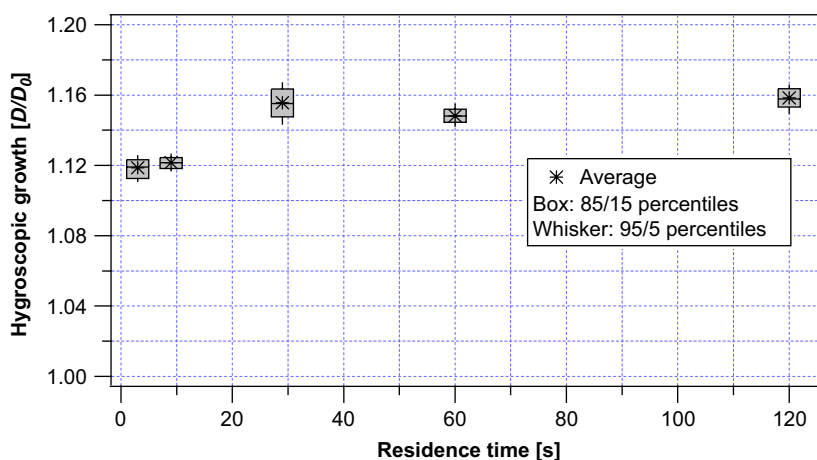


Fig. 6. Hygroscopic growth for AS/NaHA mass ratio 1:3, measured with different residence times.  $D_0 = 100$  nm and GF relates to 85% RH. Data are from the UMan HTDMA, except the 29 s data which was measured by the PSI HTDMA.

and also slightly larger than the typical deviations stated for instance in (Prenni et al., 2003), where the difference between measurement and prediction was on average 0.05 for 1:1 mixtures of ammonium sulfate and dicarboxylic acids at 90% RH. The 1:3 AS/AA mixture was also measured by (Hämeri et al., 2002) who reported a hygroscopic growth in agreement with ZSR predictions up to about 85% RH, but at higher RH the measured growth was higher than ZSR (i.e. GF 1.3 at 90% RH).

For the 1:4 mixture the hygroscopic growth doubles when the residence time is increased from 6 to 40 s (panel D in Fig. 3). A comparison with the ZSR model shows that the observed growth is below the predicted one, indicating that even 40 s may not be sufficient to reach equilibrium. Furthermore the irregularity of the particles increases with increasing AA content (see Section 4.2), and we cannot exclude compaction of the particles as they take up water, potentially leading to mobility diameter GFs smaller than volume equivalent diameter GFs due to shape effects in this case.

### 3.4. Hygroscopicity of AS/NaHA mixture

The hygroscopicity and dependence of residence time on the water uptake was measured for an AS/NaHA mixture with mass ratio 1:3 with the HTDMA. For this mixture a small increase, 0.04 in GF, was seen as the  $\tau_{res}$  increased from 10 s to above 30 s (Fig. 6). This is close to the limits of the experimental repeatability, but as the 95/5 percentiles for this mixture are quite small, we find it worth mentioning. This would imply that some mass transfer limitations can also be expected in the presence of NaHA, which is an amorphous solid. In Section 4, possibilities for mechanisms are discussed, which are based on two-phase systems. We visually investigated a mixture with a 1:3 mass ratio in a vial ( $\sim 1$  g total dry products), with water added accordingly to the measured hygroscopicity at 85% RH, and found the resulting mixture to be a thick paste, with undissolved grains from the NaHA inside. Thus it seems probable that the less soluble fraction of the NaHA remains solid also at higher RH.

In Fig. 7 humidograms of the mixture and of pure NaHA can be seen. The results correspond well with another study (Badger et al., 2006). For the ZSR model, full efflorescence of AS at 35% RH was assumed. The hygroscopicity of the mixture is low compared to the ZSR relation (panel A), which was explained by Badger et al. (2006) as interactions between AS and NaHA. They investigated a range of concentrations, and we refer to their publication for further information.

## 4. Discussion on mass transfer and hygroscopicity

There are several possible reasons for the observed effect of prolonged water vapor equilibration times. This will be addressed in the following.

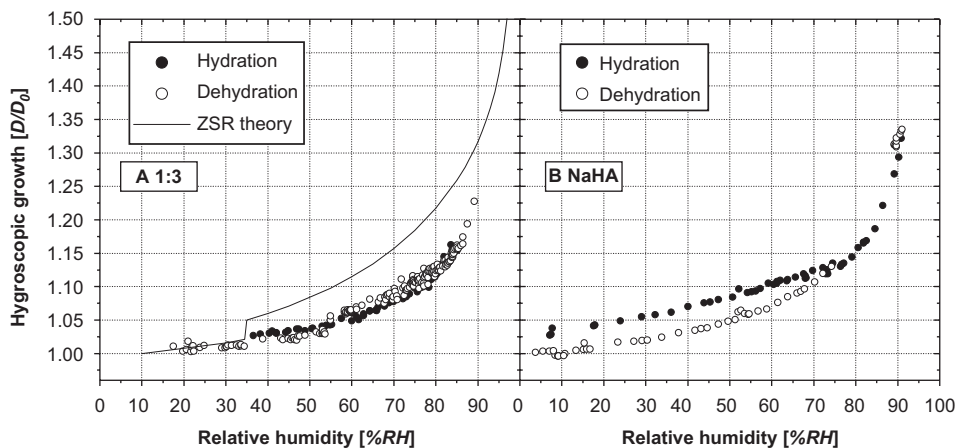


Fig. 7. Humidograms of ammonium sulfate-humic acid mixture (NaHA) from PSI HTDMA, mass ratio 1:3 (A), as well as of pure NaHA (B).  $D_0 = 100$  nm, data points measured at equilibrium.

#### 4.1. Mass transfer limitations of water vapor transport to the particle

If we consider a particle and the surrounding water vapor, the first limiting step could be the *gas diffusion* of water molecules to the particle's surface (e.g. Kerminen, 1997). These studies show that gas diffusion is fast (i.e.  $\ll 1$  s), for the conditions used here. A subsequent step is the *transfer across the gas-particle interface*. This step is seen as a thin layer where water molecules are arriving from the gas, molecules are leaving the surface back to the gas, and molecules are diffusing into the particle. The rate governing these processes is described by the accommodation coefficient,  $\alpha$ , defined as

$$\alpha = \frac{\text{number of molecules entering the liquid phase}}{\text{number of molecular collisions with the surface}}. \quad (5)$$

Under the assumptions of a spherical particle, a constant water vapor pressure, an equilibrium governed by Henry's law and a high water solubility, the accommodation coefficient,  $\alpha$ , can be approximated with the following equation (Kumar, 1989):

$$\alpha \geq \frac{R_p H_A \sqrt{2\pi M_A R T}}{3\tau_p}, \quad (6)$$

where  $R_p$  is the particle radius,  $H_A$  the Henry's law constant for water in the concentrated solution,  $M_A$  the molecular weight of water and  $\tau_p$  the time needed to obtain equilibrium.  $R$  and  $T$  are the universal gas constant and the temperature, respectively. If we consider the 1:3 mass ratio AS/AA mixture (measurements discussed in detail above), we obtain  $\tau_p = 10$  s for a particle with diameter 100 nm, for which  $\alpha$  becomes  $> 3 \times 10^{-6}$  (for  $H_A = 2.9 \text{ mol g}^{-1} \text{ atm}^{-1}$ ). Such a low mass accommodation coefficient for a liquid in contact with the gas phase is not to be expected (Chuang, 2003), thus the mass transfer is consequently assumed to be limited inside the particle. If the particle is completely liquid the *liquid diffusion* should be fast ( $\ll 1$  s for a submicrometer-sized particle consisting of a typical salt solution, if assuming a typical aqueous diffusion coefficient of  $10^{-5} \text{ cm}^2 \text{ s}^{-1}$ ). In the next section mass transfer limitations due to inhomogeneous morphology inside the particle will be discussed.

#### 4.2. Influence of morphology on hygroscopic growth and transfer limitations

The hygroscopic growth of the AS/AA mixtures presented in Section 3.4 shows deviations from the ZSR approach: for the HTDMA and the EDB measurements, the measured hygroscopic growths of the 1:3 and to a lesser extent the 1:2 mixtures are higher than predicted by the model with deviations that exceed the measurement uncertainties. Systematic changes of particle composition during the nebulizing process in the HTDMA or during the injection of a particle in

Table 2  
Solubility measurements

	Saturation solubility (mol/kg water)		Water activity $a_w$
	Adipic acid	Ammonium sulfate	
Adipic acid	$0.15 \pm 0.01$	—	$0.999 \pm 0.003$
Ammonium sulfate	—	$5.76 \pm 0.02$	$0.802 \pm 0.003$
Eutonic composition	$0.014 \pm 0.003$	$5.74 \pm 0.02$	$0.799 \pm 0.003$

the EDB seem unlikely since such an effect was not found for other particle compositions. Moreover, we verified that no AA evaporated in the HTDMA by nebulizing pure AA particles for which no change in the mobility diameter was noted during the time in the HTDMA. This is consistent with the EDB experiments which showed no weight loss of the particles over extended measurement periods.

The ZSR approach usually leads to accurate predictions of the water uptake of ammonium sulfate mixed with dicarboxylic acid mixtures (Choi & Chan, 2002; Marcolli et al., 2004). Since AA deliquesces only at 99.9% RH, we based the ZSR calculation for AS/AA mixtures on the assumption that there is no water uptake connected with the adipic acid fraction over the whole RH range. In addition to the results from the EDB as detailed above, we validated this assumption by determining the eutonic composition and the water activity of AS/AA mixtures by the methods described in Marcolli et al. (2004). The results in Table 2 show that the solubility of AA is reduced by about a factor of ten, while the one of ammonium sulfate remains unchanged within the error of the experiment. The water activity of the saturated AA solution is close to 1 while the eutonic composition deliquesces at a similar RH as AS. Moreover, we performed water activity measurements for 1:3 AS/AA aqueous suspensions in the range of  $a_w = 0.8$ –1 which showed good agreement with the ZSR model, indicating that the change of water activity due to the presence of dissolved or crystalline (particle sizes of a few micrometers) AA is below the detection limit. These bulk measurements confirm the findings from the EDB that AA remains crystalline over the whole measured humidity range.

In the following, we explore the possibility that the high water uptake of the 1:2 and 1:3 and the low one of the 1:4 AS/AA mixtures are due to morphological effects. SEM images were taken (Fig. 8) showing that under dry conditions the AS/AA mixed particles consist of a conglomerate of nanocrystals with irregular shapes, with cracks, pores and veins with diameters of 20–100 nm between them. When the DRH of ammonium sulfate is reached, it can be assumed that these pores and veins between the crystals fill with aqueous ammonium sulfate, because water molecules diffusing to the opening of a vein would more easily adsorb to the concave vein wall than the convex particle surface. The water uptake in such pores and veins is enhanced compared to the one of a flat surface or the convex particle surface. The enhancement depends on the vein diameter, determining the concavity of the liquid surface at the opening of the vein, and results in a Kelvin effect that is inverse compared to a convex liquid droplet. We denote this in the following with “inverse Kelvin effect” (Kärcher & Lohmann, 2003; Weingartner, Burtscher, & Baltensperger, 1997), as we describe the increased water uptake of the capillary due to the concave solution surface. The inverse Kelvin effect can be described by the standard Kelvin equation, with the difference that the water activity has to be divided by the Kelvin factor to obtain the equilibrium RH (Eq. (7)). To explore the influence of this effect, we calculated the water uptake for a 1:3 AS/AA particle with vein systems of varying lengths. Assuming that the liquid portion of the particle is present totally in veins and keeping the length of the vein system constant with increasing RH, the veins have to increase in diameter to accommodate the increasing solution volume (for a schematic drawing, see Fig. 9). Thus, for a fixed length of the vein system and any given solution volume, the solution concentration (i.e. the Raoult effect) as well as the vein diameter assuming veins with circular cross sections (i.e. the Kelvin effect) is given and the equilibrium RH above the vein can be calculated by

$$RH = a_w \cdot e^{-4\sigma_{\text{Sol}} \bar{V}_w \cos \phi / D_v RT} \quad (7)$$

In this equation  $a_w$  is the water activity calculated from the GF of a pure AS particle as parameterized in Eq. (4),  $\sigma_{\text{Sol}}$  is the surface tension of the solution,  $\bar{V}_w$  the partial molar volume of water,  $D_v$  the vein diameter,  $\phi$  the contact angle between the solution and the vein surface,  $R$  the ideal gas constant and  $T$  the absolute temperature. For simplicity, we calculated the vein diameter  $D_v$  assuming that AS is totally dissolved and AA totally insoluble and approximated the

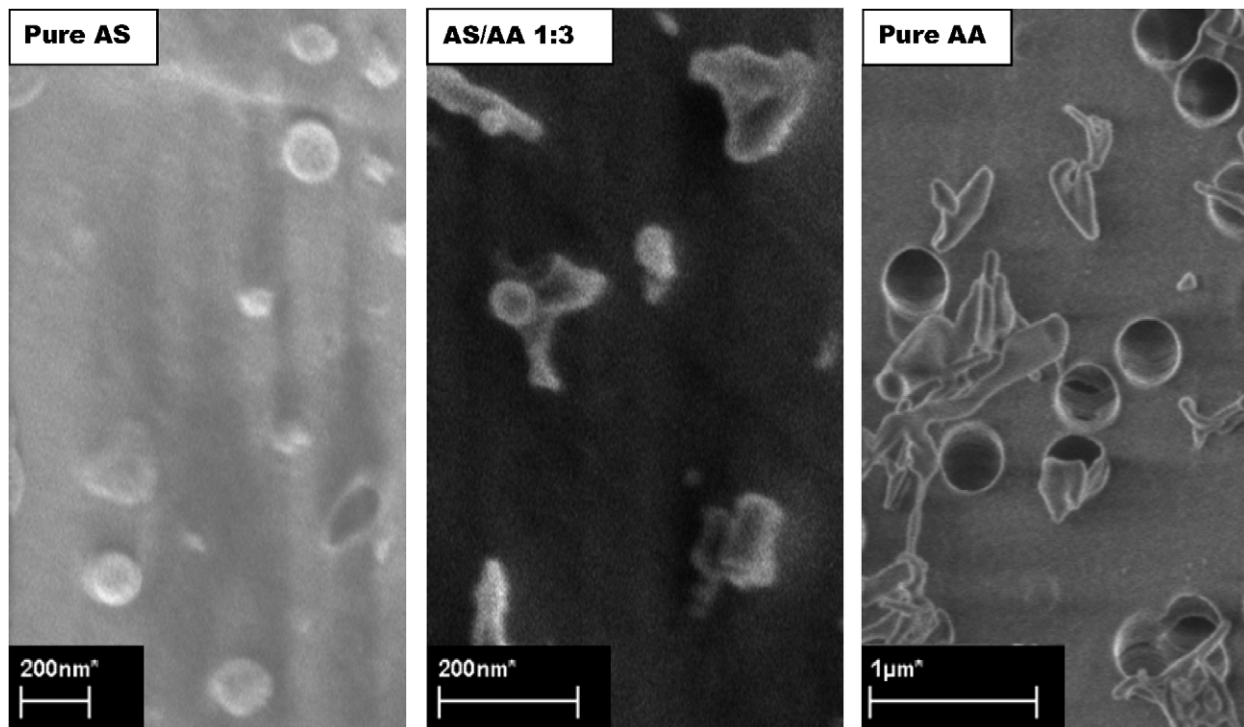


Fig. 8. SEM images of spherical pure ammonium sulfate particles, irregular particles of the 1:3 ammonium sulfate/adipic acid mixture and pure adipic acid (from left to right). The dark spherical features in the pure AA frame are the holes of the Nuclepore filter and not deposited particles.

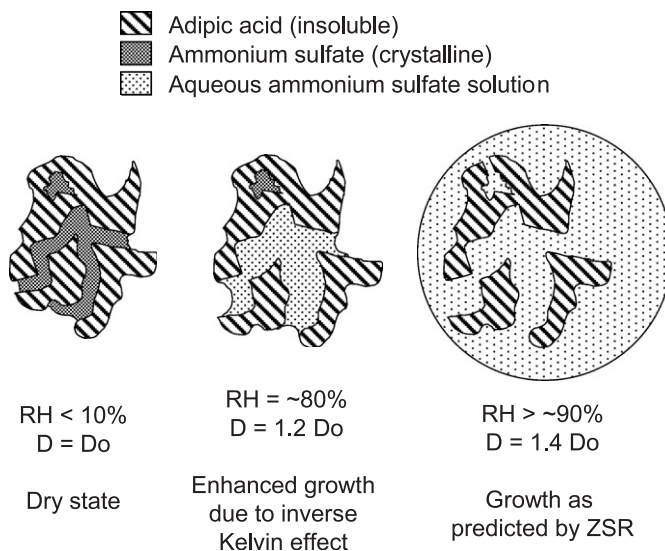


Fig. 9. Schematic drawing of the process resulting in an inverse Kelvin effect.

surface tension of the solution by the one of water. Moreover, we assumed that the solution is completely wetting the vein surface ( $\phi = 0^\circ$ ). This assumption is in accordance with Raymond and Pandis (2002).

In Fig. 10 the water uptake for a 100 nm diameter 1:3 AS/AA particle with a vein system of a total length of 400 nm is compared to the HTDMA measurement. This vein system length is compatible with a particle consisting of about

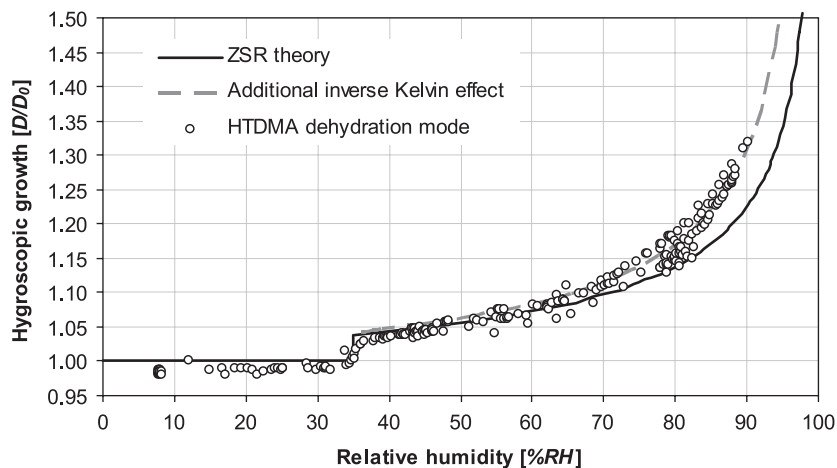


Fig. 10. HTDMA measurements of the 1:3 AS/AA mixture with the water uptake modeled with the ZSR relation, as well as modeled with the additional water uptake of an inverse Kelvin effect from a 400 nm length vein system.

eight AA crystallites with  $\sim 50$  nm diameters. The inverse Kelvin effect leads to an enhanced water uptake above 50% RH. From 50% to 90% RH the vein diameter increases from 26 to 50 nm. These diameters have to be considered as upper limits, since in our model description, we assume that all the liquid is present in veins. In reality, it will be present in grain boundaries, triple junctions as well as veins, resulting in smaller vein diameters for the same water uptake. We assume that above a critical upper value of RH the solution volume can no longer be accommodated within the veins and the inverse Kelvin effect vanishes. This upper limit does not seem to be reached yet for the 1:3 mixture, while in the case of the 1:2 mixture the slightly increased water uptake around 80% RH might indicate an inverse Kelvin effect which vanishes again at higher RH.

The inverse Kelvin effect also leads to a decrease of the DRH. For the vein system of a total length of 400 nm, a decrease of the DRH from 80.8% to 76% RH is expected. A slight decrease of DRH was observed for the particle in the EDB, and a DRH of 78.8% RH was measured with the HTDMA for the AS/AA 1:3 mixture. We assume that after efflorescence the AS crystals are present in the veins or even totally enclosed by AA (see Fig. 9). Due to capillary forces, water can enter the veins and dissolve AS partly before the DRH is reached, as can be seen from the mass increase of the particles in the EDB starting at 50% RH. This partial dissolution is limited by the space available in the vein system and might be accompanied by a transport of AS out of the veins where it recrystallizes because the inverse Kelvin effect is no longer present. We assume that before the veins can start to grow in diameter, they have to be filled completely with solution because adhesion forces between crystals impede the expansion. Full deliquescence would therefore in this case only be reached at an RH closer to the one in the absence of a Kelvin effect.

We think that the long residence times needed in the HTDMA to reach full hygroscopic growth is due to the presence of AS in veins or even totally enclosed by AA. While the spreading of the solution in the veins should not be slowed down considerably as long as the solution is wetting the vein surface (Liu, Wang, Wu, & Zhang, 2005), the expansion of the veins in diameter might be the rate limiting step. Alternatively, in the case of a total enclosure, the AA forms a barrier that has to be overcome by the water molecules leading to a slow humidification. This effect seems to be stronger the higher the AA fraction is. The characteristic time for diffusion through the solid organic matrix can be described with:

$$\tau_p = \frac{R_p^2}{\pi^2 D_{\text{Sol}}} \quad (8)$$

where  $R_p$  is the particle radius,  $D_{\text{Sol}}$  the solid diffusion coefficient and  $\tau_p$  the characteristic time needed to reach equilibrium. If we calculate  $D_{\text{Sol}}$ , again for a 100-nm diameter particle and  $\tau_p = 10$  s, we obtain  $8.0 \times 10^{-13} \text{ cm}^2 \text{ s}^{-1}$ . This is a value in the range for solids, but would in our case only be applicable to a part of the particle. If water must diffuse through this solid matrix to dissolve the AS into ions that participate in the hygroscopic growth, a fraction of the equilibration times measured can be explained.

## 5. Conclusions

Some of the inorganic/organic mixed-phase solutions studied with two HTDMAs in the present work required residence times of  $> 40$  s in order for the particles to reach equilibrium after water uptake. It is proposed that in these cases the organic compound, when present in major fractions, is solid (verified with an EDB) and encapsulates some of the inorganic species residing in between the solid organic grains in veins and pores. The water uptake rate of the mainly inorganic solution is possibly slowed down by solid phase diffusion. It is important for measurements of such mixtures to allow for a sufficient residence time at the specified humidity for the system to equilibrate. Otherwise, the resulting underestimation of the hygroscopicity may have implications for derived aerosol properties such as light scattering (direct aerosol effect in climate considerations) and cloud activation (indirect aerosol effect).

## Acknowledgments

This work was supported by the National Science Foundation Switzerland (Grant no 200021-100280) as well as the EC project ACCENT. The UMan measurements were supported by the UK Natural Environment Research Council (Grant no NER/A/S/2001/01135). M.J. Cubison was supported during the period of this work through NERC studentship no. 06424. We gratefully acknowledge the Laboratory for Micro- and Nanotechnology and A. Weber for the SEM (Zeiss Supra55VP) micrographs (PSI, Switzerland). We appreciate the inspiring exchange of ideas with Marcia Baker (University of Washington, USA).

## References

- Ansari, A. S., & Pandis, S. N. (1999). Prediction of multicomponent inorganic atmospheric aerosol behavior. *Atmospheric Environment*, 33(5), 745–757.
- Badger, C. L., George, I., Griffiths, P. T., Braban, C. F., Cox, R. A., & Abbatt, J. P. D. (2006). Phase transitions and hygroscopic growth of aerosol particles containing humic acid and mixtures of humic acid and ammonium sulphate. *Atmospheric Chemistry and Physics*, 6, 755–768.
- Biskos, G., Paulsen, D., Russell, L. M., Buseck, P. R., & Martin, S. T. (2006). Prompt deliquescence and efflorescence of aerosol nanoparticles. *Atmospheric Chemistry and Physics*, 6, 4633–4642.
- Chan, M. N., & Chan, C. K. (2005). Mass transfer effects in hygroscopic measurements of aerosol particles. *Atmospheric Chemistry and Physics*, 5, 2703–2712.
- Choi, M. Y., & Chan, C. K. (2002). Continuous measurements of the water activities of aqueous droplets of water-soluble organic compounds. *Journal of Physical Chemistry A*, 106(18), 4566–4572.
- Chuang, P. Y. (2003). Measurement of the timescale of hygroscopic growth for atmospheric aerosols. *Journal of Geophysical Research-Atmospheres*, 108(D9), art. no.-4282.
- Colberg, C. A., Krieger, U. K., & Peter, T. (2004). Morphological investigations of single levitated  $\text{H}_2\text{SO}_4/\text{NH}_3/\text{H}_2\text{O}$  aerosol particles during deliquescence/efflorescence experiments. *Journal of Physical Chemistry A*, 108(14), 2700–2709.
- Colberg, C. A., Luo, B. P., Wernli, H., Koop, T., & Peter, T. (2003). A novel model to predict the physical state of atmospheric  $\text{H}_2\text{SO}_4/\text{NH}_3/\text{H}_2\text{O}$  aerosol particles. *Atmospheric Chemistry and Physics*, 3, 909–924.
- Cubison, M. J. (2005). *Design, construction and use of a hygroscopic tandem differential mobility analyser*. Ph.D. thesis, University of Manchester, Manchester.
- Cubison, M. J., Coe, H., & Gysel, M. (2005). A modified hygroscopic tandem DMA and a data retrieval method based on optimal estimation. *Journal of Aerosol Science*, 36(7), 846–865.
- Davis, E. J., Buehler, M. F., & Ward, T. L. (1990). The double-ring electrodynamic balance for microparticle characterization. *Review of Scientific Instruments*, 61(4), 1281–1288.
- Dick, W. D., Saxena, P., & McMurry, P. H. (2000). Estimation of water uptake by organic compounds in submicron aerosols measured during the Southeastern Aerosol and Visibility Study. *Journal of Geophysical Research Atmospheres*, 105(D1), 1471–1479.
- Graber, E. R., & Rudich, Y. (2006). Atmospheric HULIS: How humic-like are they? A comprehensive and critical review. *Atmospheric Chemistry and Physics*, 6, 729–753.
- Gysel, M., Weingartner, E., & Baltensperger, U. (2002). Hygroscopicity of aerosol particles at low temperatures. 2. Theoretical and experimental hygroscopic properties of laboratory generated aerosols. *Environmental Science & Technology*, 36(1), 63–68.
- Gysel, M., Weingartner, E., Nyeki, S., Paulsen, D., Baltensperger, U., Galambos, I. et al. (2004). Hygroscopic properties of water-soluble matter and humic-like organics in atmospheric fine aerosol. *Atmospheric Chemistry and Physics*, 4, 35–50.
- Hämeri, K., Charlson, R., & Hansson, H. C. (2002). Hygroscopic properties of mixed ammonium sulfate and carboxylic acids particles. *AIChE Journal*, 48(6), 1309–1316.
- Hennig, T., Massling, A., Brechtel, F. J., & Wiedensohler, A. (2005). A tandem DMA for highly temperature-stabilized hygroscopic particle growth measurements between 90% and 98% relative humidity. *Journal of Aerosol Science*, 36(10), 1210–1223.
- IPCC (2001). *Climate change 2001: The scientific basis*, Cambridge University Press, New York.

- Joutsensaari, J., Vaattovaara, P., Vesterinen, M., Hämeri, K., & Laaksonen, A. (2001). A novel tandem differential mobility analyzer with organic vapor treatment of aerosol particles. *Atmospheric Chemistry and Physics*, *1*, 51–60.
- Kanakidou, M., Seinfeld, J. H., Pandis, S. N., Barnes, I., Dentener, F. J., Facchini, M. C. et al. (2005). Organic aerosol and global climate modelling: a review. *Atmospheric Chemistry and Physics*, *5*, 1053–1123.
- Kärcher, B., & Lohmann, U. (2003). A parameterization of cirrus cloud formation: heterogeneous freezing. *Journal of Geophysical Research*, *108*(D14), 4402–4416.
- Kerminen, V. M. (1997). The effects of particle chemical character and atmospheric processes on particle hygroscopic properties. *Journal of Aerosol Science*, *28*(1), 121–132.
- Kiss, G., Tombacz, E., Varga, B., Alsberg, T., & Persson, L. (2003). Estimation of the average molecular weight of humic-like substances isolated from fine atmospheric aerosol. *Atmospheric Environment*, *37*(27), 3783–3794.
- Krieger, U. K., & Braun, C. (2001). Light-scattering intensity fluctuations in single aerosol particles during deliquescence. *Journal of Quantitative Spectroscopy & Radiative Transfer*, *70*(4–6), 545–554.
- Kumar, S. (1989). The characteristic time to achieve interfacial phase equilibrium in cloud drops. *Atmospheric Environment*, *23*, 2299–2304.
- Liu, Y. C., Wang, Q., Wu, T., & Zhang, L. (2005). Fluid structure and transport properties of water inside carbon nanotubes. *Journal of Chemical Physics*, *123*(23).
- Marcolli, C., Luo, B. P., & Peter, T. (2004). Mixing of the organic aerosol fractions: Liquids as the thermodynamically stable phases. *Journal of Physical Chemistry A*, *108*(12), 2216–2224.
- McFiggans, G., Artaxo, P., Baltensperger, U., Coe, H., Facchini, M. C., Feingold, G. et al. (2006). The effect of physical and chemical aerosol properties on warm cloud droplet activation. *Atmospheric Chemistry and Physics*, *6*, 2593–2649.
- Prenni, A. J., De Mott, P. J., & Kreidenweis, S. M. (2003). Water uptake of internally mixed particles containing ammonium sulfate and dicarboxylic acids. *Atmospheric Environment*, *37*(30), 4243–4251.
- Putaud, J. P., Raes, F., Van Dingenen, R., Brüggemann, E., Facchini, M. C., Decesari, S. et al. (2004). European aerosol phenomenology-2: Chemical characteristics of particulate matter at kerbside, urban, rural and background sites in Europe. *Atmospheric Environment*, *38*(16), 2579–2595.
- Rader, D. J., & McMurry, P. H. (1986). Application of the tandem differential mobility analyzer to studies of droplet growth or evaporation. *Journal of Aerosol Science*, *17*(5), 771–787.
- Ray, J., & McDow, S. R. (2005). Dicarboxylic acid concentration trends and sampling artifacts. *Atmospheric Environment*, *39*(40), 7906–7919.
- Raymond, T. M., & Pandis, S. N. (2002). Cloud activation of single-component organic aerosol particles. *Journal of Geophysical Research-Atmospheres*, *107*(D24), art. no.-4787.
- Russell, L. M., & Ming, Y. (2002). Deliquescence of small particles. *Journal of Chemical Physics*, *116*(1), 311–321.
- Stokes, R. H., & Robinson, R. A. (1966). Interactions in aqueous nonelectrolyte solutions. I. Solute-solvent equilibria. *Journal of Physical Chemistry*, *70*, 2126–2130.
- Tang, I. N., & Munkelwitz, H. R. (1993). Composition and temperature-dependence of the deliquescence properties of hygroscopic aerosols. *Atmospheric Environment Part a-General Topics*, *27*(4), 467–473.
- Topping, D. O., McFiggans, G. B., & Coe, H. (2005a). A curved multi-component aerosol hygroscopicity model framework: Part 1—Inorganic compounds. *Atmospheric Chemistry and Physics*, *5*, 1205–1222.
- Topping, D. O., McFiggans, G. B., & Coe, H. (2005b). A curved multi-component aerosol hygroscopicity model framework: Part 2—Including organic compounds. *Atmospheric Chemistry and Physics*, *5*, 1223–1242.
- Vlasenko, A., Sjogren, S., Weingartner, E., Stemmler, K., Gäggeler, H. W., & Ammann, M. (2006). Effect of humidity on nitric acid uptake to mineral dust aerosol particles. *Atmospheric Chemistry and Physics*, *6*, 2147–2160.
- Weingartner, E., Burtscher, H., & Baltensperger, U. (1997). Hygroscopic properties of carbon and diesel soot particles. *Atmospheric Environment*, *31*(15), 2311–2327.
- Weingartner, E., Gysel, M., & Baltensperger, U. (2002). Hygroscopicity of aerosol particles at low temperatures. 1. New low-temperature H-TDMA instrument: Setup and first applications. *Environmental Science and Technology*, *36*(1), 55–62.
- Winklmayr, W., Reischl, G. P., Lindner, A. O., & Berner, A. (1991). New electromobility spectrometer for the measurement of aerosol size distributions in the size range from 1 to 1000 nm. *Journal of Aerosol Science*, *22*, 289–296.